Available online at www.eccomasproceedia.org
Eccomas Proceedia COMPDYN (2023) 1697-1706

ECCOMAS
Proceedia

COMPDYN 2023
9th ECCOMAS Thematic Conference on
Computational Methods in Structural Dynamics and Earthquake Engineering
M. Papadrakakis, M. Fragiadakis (eds.)
Athens, Greece, 12-14 June 2023

GENERATIVE MODELLING AND SEISMIC ASSESSMENT OF ANCIENT TEMPLES: THE TEMPLE OF VESTA (TIVOLI)

Annalaura Vuoto[1], Marco F. Funari[2], Shaghayegh Karimzadeh[1], and Paulo B. Lourenço[1]

[1] ISISE, Department of Civil Engineering, University of Minho Campus de Azurém, 4800-058 Guimarães, Portugal
e-mail: annalauravuoto1307@gmail.com, shaghkn@civil.uminho.pt, pbl@civil.uminho.pt

[2] School of Sustainability, Civil and Environmental Engineering, University of Surrey, Guildford GU2 7XH, UK
m.funari@surrey.ac.uk

Abstract

This paper proposes an innovative procedure to generate digital models of architectural heritage, assuming the unavailability of geometrical information such as point clouds. The Temple of Vesta in Tivoli is adopted as a case study, whereas the etchings performed by Francesco Piranesi in the XVIII century are used to identify the architectural layout, modules' repetitions etc. Hence, a Generative Program (GP) algorithm is implemented for the temple parametrisation. The geometrical model is imported and treated as a concurrent continuous/block-based model in a Finite Element environment and adopted to perform nonlinear time history simulations. Seven seismic records with two horizontal components are selected and scaled according to the target spectrum of the Italian seismic code at the limit state Safeguard of human life. Simulations are performed considering the structure at its not retrofitted state (i.e. anchorages and steel elements connections are not taken into account). The numerical model underlines how local failure mechanisms of columns and entablature always affect the structure.

Keywords: Ancient Temple, Parametric Modelling, Ground Motion Selection and Scaling Seismic Vulnerability.

ISSN:2623-3347 © 2023 The Authors. Published by Eccomas Proceedia.
Peer-review under responsibility of the organizing committee of COMPDYN 2023.
doi: 10.7712/120123.10512.20725

1 INTRODUCTION

In the last few decades, impressive advancements have been made in the digitalisation and modelling of architectural heritage. Nowadays, equipment and digital tools permit the full reconstruction of complex geometry integrating within Historic Building Information Modelling (HBIM) and Digital Twinning workflows. However, sometimes engineers face the issue of performing the numerical modelling of heritage buildings with limited accessibility due to unforeseen circumstances or even with assets that are entirely or partially collapsed [1]. Parametric-based modelling approaches may be a valuable tool for performing geometrical modelling of heritage buildings characterised by architectural layouts consisting of regular modules and repetition, architectural orders, etc. [2]. However, few applications to historic masonry buildings are present hitherto in the literature [3,4]. In such cases, multidisciplinary research might investigate the causes generating the collapse or assess the structural capacity to ensure adequate safety (i.e. opening heritage sites for tourism purposes).

High-fidelity geometrical reconstructions should be used in conjunction with appropriate numerical approaches, contributing significantly to predicting damage scenarios and, consequently, structural integrity safety. In the last decades, numerical models, either based on the Discrete Element Method (DEM) or Finite Element Method (FEM), have been extensively used for nonlinear dynamic analysis of Historical Masonry Structures (HMS) [5–12]. DEM is particularly suitable for modelling large displacement static or dynamics problems. Unlike time-consuming advanced methods of analysis, other methods allow users to perform a seismic assessment of masonry buildings in a rapid and computationally-efficient manner [13,14]. However, FEM is still the most used strategy because of the large spread among practitioners and researchers, despite the limitations of modelling masonry as a homogeneous material [8,15–17].

This work ambitiously aims to implement a workflow which goes from the geometrical parametrisation of ancient temples to the performance of high-fidelity nonlinear time history analyses. Section 2 briefly describes the case study, and section 3 discusses the methodology adopted. Next, section 4 presents the nonlinear dynamic simulations results, and finally, the remarkable conclusion is addressed in section 5.

2 THE VESTA TEMPLE IN TIVOLI

The Temple of Vesta (Figure 1) is part of the ancient acropolis of Tivoli (Italy), dating to the early 1st century BC.

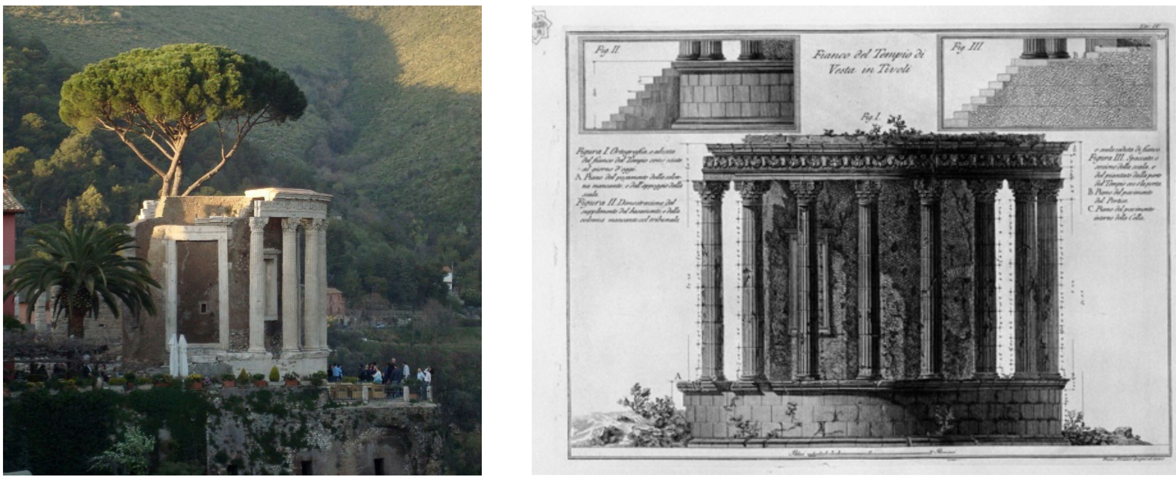

(a) (b)

Figure 1: Vesta Temple: (a) representation of its current state, (b) Piranesi's etching

Historians disagree about whom the temple was dedicated, whether to Hercules, the protecting god of Tibur, Albunea, Tiburnus, or Vesta herself. People populating that area used the temple until the 16^{th} century for different purposes, ensuring adequate maintenance that has permitted to conserve it in a decent state. In fact, the cell, even if damaged, presents its original layout. Ten out of eighteen Corinthian columns remain standing.

Across the centuries, the Vesta Temple attracted the interest of several architects who performed detailed surveys as well as hypotheses regarding the original architectural layout of the temple. Among them, it is worth to be mentioned Francesco Piranesi (Figure 1b), who developed a detailed survey of the temple, even representing the columns' blocks discretisation and hypotheses concerning the original layout, which includes a hemispherical dome surmounting the cell.

3 METHODOLOGY

Once the module repetitions and the geometrical rules adopted by the ancient masons are identified, the following step consists of translating them into a set of coding rules to get the full geometry of the structure. Hence, the geometrical model is linked with a structural software environment in which nonlinear dynamic analyses are performed by using ground motions selected and scaled according to the target response spectrum of Tivoli.

3.1 Geometrical model

Geometrical modelling is addressed by using the Generative Programming (GP) paradigm implemented in a visual programming environment. After acquiring the geometrical data (detailed, dimensioned drawings by Francesco Piranesi dating back to 1780), the geometry of the Vesta Temple is analysed to parametrically discretise it by identifying (i) entities, (ii) sub-entities, (iii) modules, repetitions, and (iv) symmetries. The proposed algorithm has been implemented within the visual programming environment offered by Rhinoceros3D + Grasshopper [18,19]. In the present study, the current state of the temple is analysed, even though the proposed tool allows one to easily switch to the original state by employing the same generative script (Figure 2).

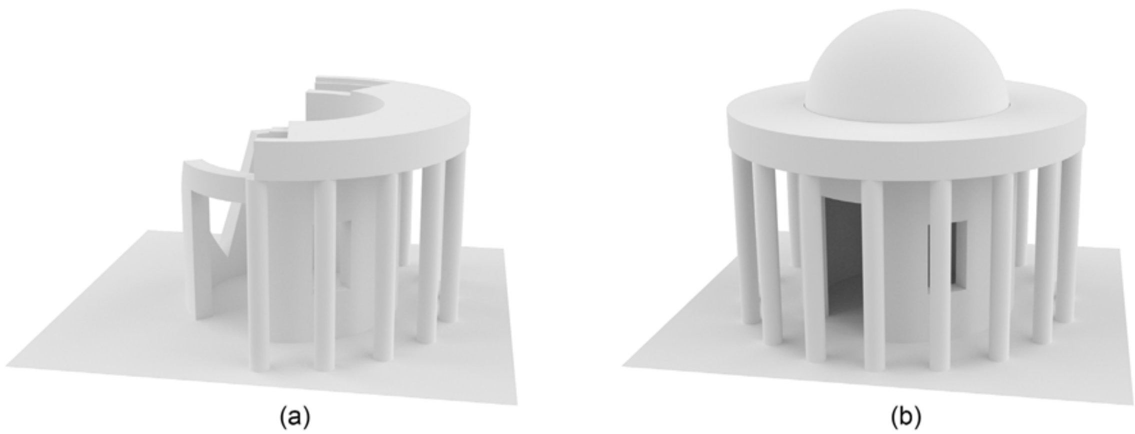

Figure 2: Geometrical model of Vesta Temple: (a) current state, (b) original state - Piranesi's hypothesis

3.2 Finite Element implementation

The structural modelling of the Temple of Vesta has been performed using a concurrent continuous/block-based approach [20]. In particular, the cell is modelled via the macro-modelling approach [21], meaning that the masonry arrangement is smeared in a homogeneous material. Masonry non-linearities have been taken into account via the so-called Concrete Damage Plasticity (CDP), which couples plasticity with a scalar-based damage model [22]. The quasi-brittle nature of masonry is represented by a linear type of softening in tension. In compression, a plateau exists after the compressive strength, followed by a linear type of softening. Damage variables are adopted when softening is active and aim at reducing the initial (undamaged) elastic modulus through the following expressions:

$$\boldsymbol{\sigma_c = (1 - d_c)E_0(\varepsilon_c - \varepsilon_c^{pl})} \quad \text{Eq. 1}$$

$$\boldsymbol{\sigma_t = (1 - d_t)E_0(\varepsilon_t - \varepsilon_t^{pl})}$$

where E_0 is the elastic modulus of the undamaged masonry, σ_i is the effective stress value; d is the damage parameter relating the effective stress with the corresponding inelastic strain, ε_i is the total strain value, and ε_i^{pl} is the inelastic (plastic) strain value. The subscript i reads as c or t, if associated with the compressive or tensile regime, respectively. A scalar-based damage model describes the damage in tension d_t (cracking) and compression d_c (crushing), which can assume a value between zero (no damage) and one (fully damaged). When cyclic loading is applied, loss of stiffness in the unloading phase due to cracking and crushing is likely to happen. CDP assumes a non-associative flow rule given as a Drucker-Prager hyperbolic function and requires the definition of physically based parameters. Material properties adopted in the numerical analysis are reported in Table 1.

Table 1: Material properties and model parameters

E_0 [MPa]	ν	ρ [kg m^{-3}]	Dilatation angle	Eccentricity	f_{b0}/f_{c0}	K_c	Viscosity parameter
1000	0.2	1450	10°	0.1	1.16	2/3	0.002

Compressive behaviour			Tensile behaviour		
Stress [MPa]	Inelastic strain	d_c	Stress [MPa]	Inelastic strain	d_t
2.00	0	0	0.15	0	0
2.20	0.004	0	0.001	0.002	0.9
0.2	0.010	0.9	0.001	0.010	0.9
0.2	0.020	0.9	-	-	-

Considering the aim of the proposed work, which is to perform a safety assessment of the temple, viscous damping has been neglected for a conservative assessment [23].

Travertine blocks, forming the columns, ceiling and entablature, are assumed to be deformable discrete blocks following an isotropic and linear elastic constitutive law ($\mathrm{E} = 63\ GPa, \mathrm{\nu} = 0.2$). The dry-assemblage of blocks is represented by zero-thickness interfaces, which include a non-associative plastic flow rule and a classical Mohr-Coulomb failure surface criterion. Normal and tangential contact behaviours assume an infinitesimal interpenetration between blocks. A linear relationship between the over-closure displacements and the applied stress is defined by the normal and tangential stiffness values of $k_n = 5 \times 10^9$ Pa/m and $k_s = 2 \times 10^9$ Pa/m, respectively. A friction coefficient ($f = 0.70$) defines the plastic slipping criterion in shear within a penalty approach, in which a perfectly plastic response occurs after reaching the critical shear stress. There is no viscous damping set to the contact since the present research is concerned about the stability of the structures, which is not critically sensitive to the damping [23].

The three-dimensional FE model (Figure 3) enforces the use of three-dimensional (solid) solid elements; therefore, the mesh discretisation is achieved using tetrahedron FEs for the cell (TETC3D4) and hexahedral FEs for the remaining structural components (C3D8R).

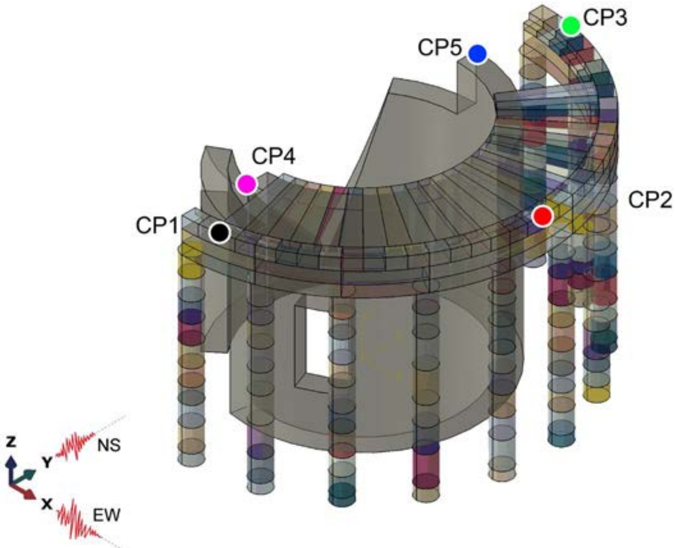

Figure 3: FE discretisation: geometry, boundary and loading conditions

Appropriate boundary and loading conditions have been implemented to perform the seismic assessment. Numerical analyses have been performed by applying two phases that idealised the load process: at first, the gradual application of gravity loads and, subsequently, ground motion records simultaneously in North-South (NS) (Y) and East-West (EW) (X) directions. To integrate the equation of motion, an explicit time integration scheme has been adopted with nonlinear geometries taken into consideration [24].

3.3 Ground Motion Selection and Scaling

In this study, seven records with two horizontal components (NS and EW) have been selected and scaled in the time domain according to the target spectrum of the Italian seismic code [25] calculated for the *limit state Safeguard of human life*. This limit state corresponds to the return period of 475 years which is consistent with the 10% probability of exceedance in a nominal life of 50 years. The selection process criterion is the mean of the square root of the sum of squares (SRSS) of the Pseudo-Spectral Acceleration (pSa) for two horizontal components of the selected records within the period range of $0.5\ s$ to a maximum of $2.0\ s$ and $1.5 \times \mathrm{T}_1$, where T_1 is the fundamental period of the structure, should be between 90% and 130% of the target spectrum. Additionally, the mean spectra for the selected motions at $\mathrm{T} = 0$ s must not be less than the target spectral amplitude at the site of interest.

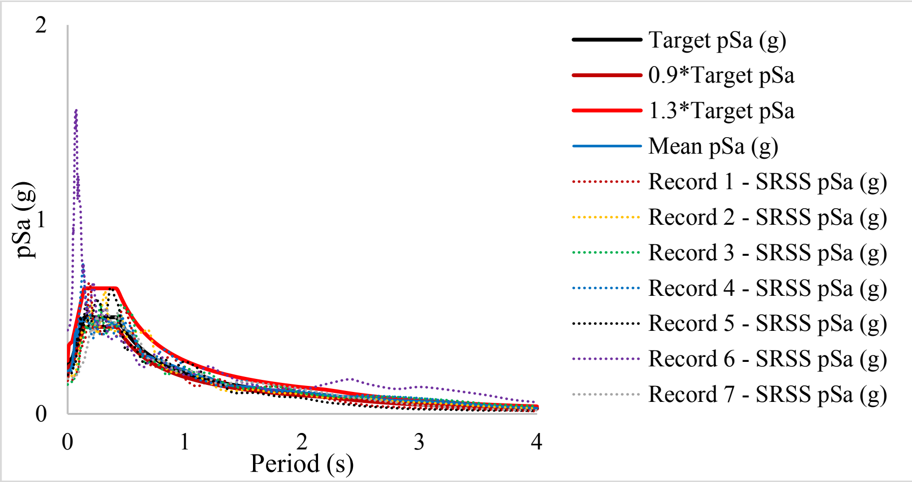

Figure 4: Comparison of the individual and mean spectra corresponding to the selected records with the target spectra at the site of interest.

The information in the target structure determines the seismological selection criteria. According to the region, the magnitude is confined to earthquakes between M_w=5.5 and M_w=7.5, with a normal and reverse faulting mechanism recorded at stations with an epicentral distance of 50 to 150 km. The soil class of the temple is assumed type B; hence, only ground motions recorded on soil type B with V_{s30} ranging from 360 to 760 m/s are used in the selection process. Through the PEER ground motion selection platform, the scaling procedure is performed by minimising the mean square error [26]. To this end, the maximum scaling factor is limited to 5.0. Figure 4 compares the target spectra with the individual and the mean spectra of the selected records at the site of interest.

4 RESULTS

This section discusses the results of the nonlinear dynamic analyses. Seven nonlinear dynamic analyses have been performed, and results in terms of response measures are compared. Specifically, control points' displacement and the maximum base shear are analysed.

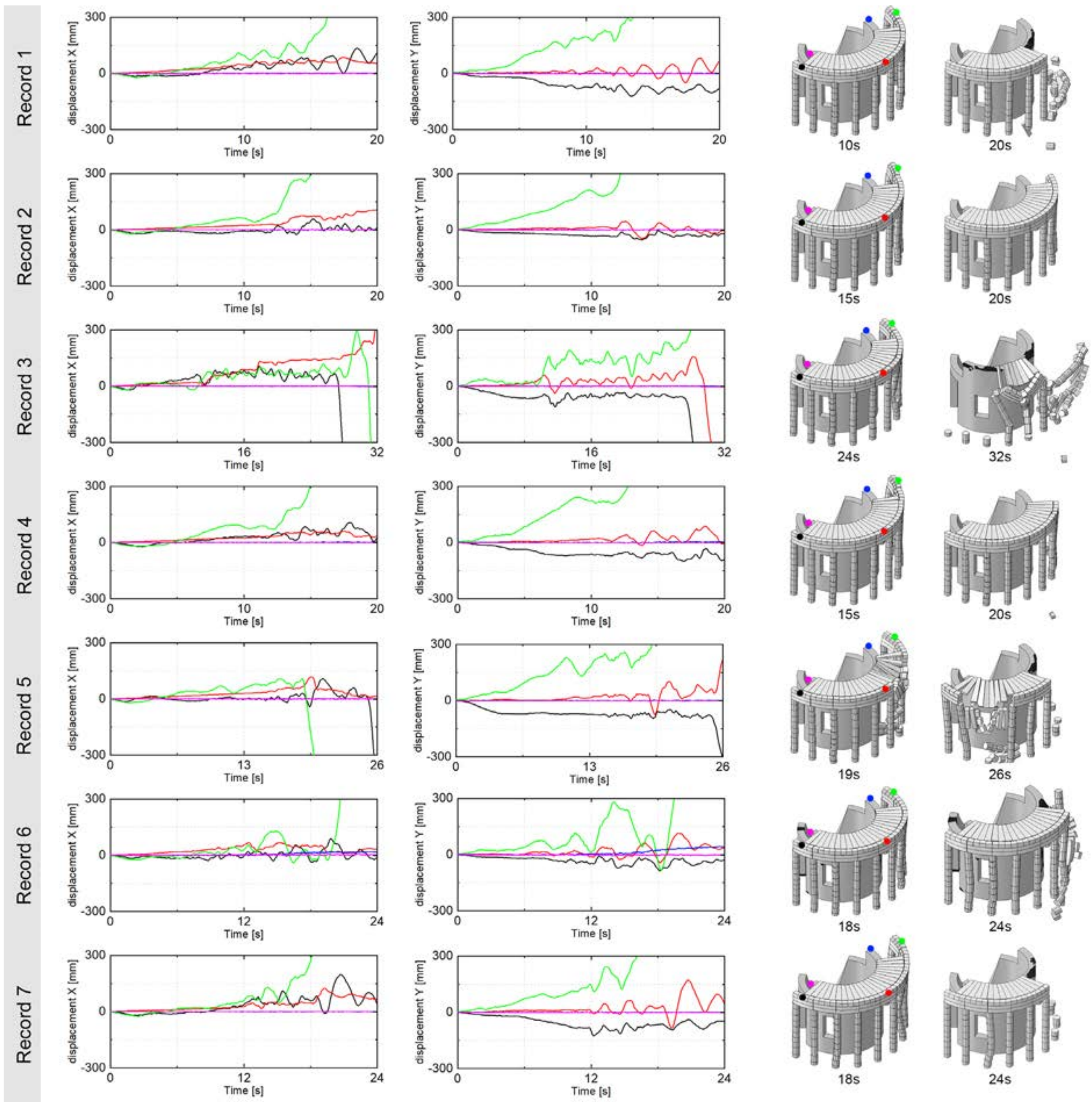

Figure 5: Time history displacement of selected control points (different colours) and failure mechanisms

Figure 5 represents the displacement time histories obtained for the considered ground motion records. Displacements of control points located on top of the entablature and cell have been monitored. All the simulations end up with a local failure mechanism involving columns and entablature, whereas the cell is unlikely to be damaged, and the control point presents a negligible displacement compared to those located on the top of the entablature. The maximum base shear for each direction is reported in Figure 6. The results are normalised for the gravity loads. One should note how the results are consistent except for Record 5, which presents a base shear magnitude (Y direction) four times greater than the overall trend. This can be attributed to Record 5 higher spectral amplitudes around the fundamental period of the structure, see Figure 4.

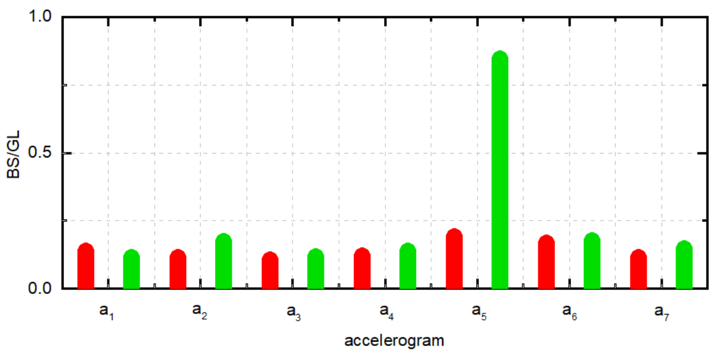

Figure 6: FE maximum base shear in X (red), and Y (green) directions

5 CONCLUSION

This paper presents a workflow implemented in a Generative Programming environment that drives the definition of geometrical modelling of architectural heritage characterised by symmetries, repetition of modules and architectural orders, intending to make the process fast and efficient.

The Vesta Temple of Tivoli is adopted as a case study. Specifically, a seismic assessment has been performed by implementing a concurrent continuum/block-based approach. Seven records with two horizontal components have been selected and scaled according to the target spectrum of the Italian seismic code at the *limit state Safeguard of human life*.

From this study, the following conclusions are derived:

- Historic documentation may be a valuable source of information for assessing the structural performance of heritage structures that are ruined state.
- GP paradigm is an efficient approach for developing the geometrical model of structures which present symmetries, repetition of modules, etc.
- The proposed tool is flexible and can easily reproduce the geometrical definition of other monopteros temples in no time.
- Nonlinear dynamic analyses underline how the lack of connection between the cell and columns is the main source of failures due to alternative ground motion shakings.

Future developments will include (i) modelling the retrofitted configuration (i.e. considering steel and tie connection present at the current state) to evaluate their efficiency, (ii) investigating the original configuration of the temple to frame some hypotheses regarding the cause of its current damaged state.

ACKNOWLEDGEMENTS

This study is partly funded by the STAND4HERITAGE project (New Standards for Seismic Assessment of Built Cultural Heritage) which has received funding from the European Research Council (ERC) under the European Union's Horizon 2020 research and innovation program (Grant Agreement No. 833123) as an Advanced Grant. This work is also partly financed by MPP2030-FCT PhD Grants under the R&D Unit Institute for Sustainability and Innovation in Structural Engineering (ISISE), under reference PRT/BD/152822/2021.

REFERENCES

[1] M. Stepinac, M. Gašparović, A review of emerging technologies for an assessment of safety and seismic vulnerability and damage detection of existing masonry structures, Appl. Sci. 10 (2020) 5060.

[2] M. Calvano, L. Martinelli, F. Calcerano, E. Gigliarelli, Parametric Processes for the Implementation of HBIM—Visual Programming Language for the Digitisation of the Index of Masonry Quality, ISPRS Int. J. Geo-Information 2022, Vol. 11, Page 93. 11 (2022) 93. https://doi.org/10.3390/IJGI11020093.

[3] D.M.S. Paulino, R. Napolitano, H. Ligler, E. Hill, A Grammar-Based Methodology to Support the Adaptive Reuse of Historic Buildings, (2021).

[4] M.F. Funari, A.E. Hajjat, M.G. Masciotta, D. V. Oliveira, P.B. Lourenço, A Parametric Scan-to-FEM Framework for the Digital Twin Generation of Historic Masonry Structures, Sustain. 2021, Vol. 13, Page 11088. 13 (2021) 11088. https://doi.org/10.3390/SU131911088.

[5] B. Pulatsu, S. Gonen, F. Parisi, E. Erdogmus, K. Tuncay, M.F. Funari, P.B. Lourenço, Probabilistic approach to assess URM walls with openings using discrete rigid block analysis (D-RBA), J. Build. Eng. 61 (2022) 105269. https://doi.org/https://doi.org/10.1016/j.jobe.2022.105269.

[6] M.F. Funari, B. Pulatsu, S. Szabó, P.B. Lourenço, A Solution for the Frictional Resistance in Macro-Block Limit Analysis of Non-periodic Masonry, STRUCTURES. (2022).

[7] A.M. D'altri, V. Sarhosis, G. Milani, J. Rots, S. Cattari, S. Lagomarsino, E. Sacco, A. Tralli, G. Castellazzi, S. De Miranda, Modeling Strategies for the Computational Analysis of Unreinforced Masonry Structures: Review and Classification, 27 (2020) 1153–1185. https://doi.org/10.1007/s11831-019-09351-x.

[8] V. Sarhosis, J. V Lemos, K. Bagi, Chapter 13 - Discrete element modeling, in: B. Ghiassi, G.B.T.-N.M. of M. and H.S. Milani (Eds.), Woodhead Publ. Ser. Civ. Struct. Eng., Woodhead Publishing, 2019: pp. 469–501. https://doi.org/https://doi.org/10.1016/B978-0-08-102439-3.00013-0.

[9] M.F. Funari, S. Spadea, P. Lonetti, F. Fabbrocino, R. Luciano, Visual programming for structural assessment of out-of-plane mechanisms in historic masonry structures, J. Build. Eng. 31 (2020). https://doi.org/10.1016/j.jobe.2020.101425.

[10] N. Hoveidae, A. Fathi, S. Karimzadeh, Seismic damage assessment of a historic masonry building under simulated scenario earthquakes: A case study for Arge-Tabriz, Soil Dyn. Earthq. Eng. 147 (2021) 106732. https://doi.org/https://doi.org/10.1016/j.soildyn.2021.106732.

[11] A.Y. Elghazouli, D. V Bompa, S.A. Mourad, A. Elyamani, In-plane lateral cyclic behaviour of lime-mortar and clay-brick masonry walls in dry and wet conditions, Bull. Earthq. Eng. 19 (2021) 5525–5563.

[12] Y.T. Guo, D. V Bompa, A.Y. Elghazouli, Nonlinear numerical assessments for the in-plane response of historic masonry walls, Eng. Struct. 268 (2022) 114734. https://doi.org/https://doi.org/10.1016/j.engstruct.2022.114734.

[13] M.F. Funari, A. Mehrotra, P.B. Lourenço, A tool for the rapid seismic assessment of historic masonry structures based on limit analysis optimisation and rocking dynamics, Appl. Sci. 11 (2021) 1–22. https://doi.org/10.3390/app11030942.

[14] A. Mehrotra, M.J. DeJong, A CAD-interfaced dynamics-based tool for analysis of masonry collapse mechanisms, Eng. Struct. 172 (2018) 833–849. https://doi.org/10.1016/j.engstruct.2018.06.053.

[15] E. Bertolesi, L.C. Silva, G. Milani, Validation of a two-step simplified compatible homogenisation approach extended to out-plane loaded masonries, Int. J. Mason. Res. Innov. 4 (2019) 265. https://doi.org/10.1504/IJMRI.2019.10019407.

[16] M.F. Funari, L.C. Silva, E. Mousavian, P.B. Lourenço, Real-time Structural Stability of Domes through Limit Analysis: Application to St. Peter's Dome, Https://Doi.Org/10.1080/15583058.2021.1992539. (2021) 1–23. https://doi.org/10.1080/15583058.2021.1992539.

[17] F. Clementi, A. Ferrante, E. Giordano, F. Dubois, S. Lenci, Damage assessment of ancient masonry churches stroked by the Central Italy earthquakes of 2016 by the non-smooth contact dynamics method, Bull. Earthq. Eng. 18 (2020) 455–486. https://doi.org/10.1007/S10518-019-00613-4.

[18] Rhino—Rhinoceros 3D. 2020, (2020).

[19] Grasshopper—Algorithmic Modeling for Rhino. 2020, (2020).

[20] M.F. Funari, L.C. Silva, N. Savalle, P.B. Lourenço, A concurrent micro/macro FE-model optimized with a limit analysis tool for the assessment of dry-joint masonry structures, Int. J. Multiscale Comput. Eng. In Press (2022). https://doi.org/10.1615/IntJMultCompEng.2021040212.

[21] G. Fortunato, M.F. Funari, P. Lonetti, Survey and seismic vulnerability assessment of the Baptistery of San Giovanni in Tumba (Italy), J. Cult. Herit. xxx (2017). https://doi.org/10.1016/j.culher.2017.01.010.

[22] J. Lubliner, J. Oliver, S. Oller, E. Oñate, A plastic-damage model for concrete, Int. J. Solids Struct. 25 (1989) 299–326. https://doi.org/10.1016/0020-7683(89)90050-4.

[23] E. Erdogmus, B. Pulatsu, A. Gaggioli, M. Hoff, Reverse engineering a fully collapsed ancient roman temple through geoarchaeology and DEM, Int. J. Archit. Herit. 15 (2021) 1795–1815.

[24] V. Abaqus, 6.14 Documentation, Dassault Syst. Simulia Corp. 651 (2014).

[25] N. Mordà, A. Mancini, Norme tecniche per le costruzioni (NTC 2018) D. Min. Infrastrutture e Trasporti 17 gennaio 2018, (2018).

[26] T.D. Ancheta, R.B. Darragh, J.P. Stewart, E. Seyhan, W.J. Silva, B.S.-J. Chiou, K.E. Wooddell, R.W. Graves, A.R. Kottke, D.M. Boore, NGA-West2 database, Earthq. Spectra. 30 (2014) 989–1005.